Ninth International Conference on
THIN-WALLED STRUCTURES – ICTWS2023
Sydney, Australia, Nov 29 – Dec 1, 2023

NEW DESIGN APPROACH FOR COLD-FORMED STEEL MEMBERS SUBJECTED TO COMBINED AXIAL COMPRESSIVE LOAD AND BENDING

Maryam Hasanali[1], Seyed Mohammad Mojtabaei[2], James B.P. Lim[1,3], G.Charles Clifton[4], and Iman Hajirasouliha[5]

[1] Department of Civil and Environmental Engineering, The University of Auckland, New Zealand, and [2] School of Architecture, Building and Civil Engineering, Loughborough University, Leicestershire LE11 3TU, UK
e-mails: mhas455@aucklanduni.ac.nz, smmojtabaei1@sheffield.ac.uk

[3] School of Engineering, The University of Waikato, Hamilton, New Zealand
e-mail: jlim@waikato.ac.nz

[4] Department of Civil and Environmental Engineering, The University of Auckland, New Zealand
e-mail: c.clifton@auckland.ac.nz

[5] Department of Civil and Structural Engineering, The University of Sheffield, Sheffield S1 3JD, UK
e-mail: i.hajirasouliha@sheffield.ac.nz

Keywords: Cold-formed steel (CFS); Beam-columns; Interaction formula; Finite Element (FE) model.

Abstract. *The presented study aims to develop more accurate design equations for cold-formed steel (CFS) beam-columns under various combinations of compression and biaxial bending. To this end, experimentally validated finite element (FE) models of CFS elements were developed in ABAQUS by accounting for both nonlinear material properties and geometric imperfections. The validated models were then used for a comprehensive parametric study, covering a wide range of key design parameters, such as element length, thickness, and cross-sectional dimensions under various load eccentricity levels. The results were employed to evaluate the efficiency of the interaction formula prescribed by the current design specifications, including AS/NZS-4600, AISI S-100 and Eurocode-3, in predicting the strength of CFS lipped channel beam-columns, and develop a more reliable design equation. The results indicated that while existing design methods may lead to considerably underestimated or overestimated predictions, the proposed interaction equation could considerably improve the accuracy of the strength predictions, especially in the case of medium to high slenderness CFS beam-column elements.*

1 INTRODUCTION

Over the past two decades, there has been significant growth in the utilization of cold-formed steel (CFS) structural members [1]. In comparison to the conventional hot-rolled steel products, CFS structural members have high strength-to-weight ratios and exhibit work-hardening achieved during the forming process [2]. Primary load-bearing CFS members in portal frames and stud wall systems often act as beam-columns under combined actions of axial compression and bending moments [3-5], generated by: (i) eccentric loads [6,7], (ii) combination of axial compression loads and transverse loads [1], (iii) rigidity of the connections in CFS moment-resisting systems [8,9], and (iv) nominal imperfections in the structural members [10,11].

The structural performance of CFS beam-columns has been investigated in the literature and compared to the findings obtained using the available design codes. A study conducted by Hancock and Rasmussen [12] examined the interaction behaviour of slender square hollow

sections (SHS) and thin-walled I-sections under the combined effects of compressive load and bending moment along both major and minor axes. According to the results, when welded I-sections were bent about the minor axis, the interaction diagrams exhibited convex behaviour for shorter lengths elements and concave behaviour for longer lengths elements. On the other hand, when the cross-sections were bent about the major axis, the resulting diagrams were slightly convex over a longer length, leading to failure due to flexural-torsional buckling.

Cheng et al. [13] investigated the global buckling behaviour of CFS lipped channel elements under combined actions of compression and bending along their major- and minor-axes. In another study, Torabian et al. [4,5] conducted comprehensive experimental investigations to evaluate buckling strength and failure mechanism of warping-restrained CFS beam-columns with lipped channel and Z-shaped sections under axial compression and bi-axial bending. Hence, they proposed a new design approach, in which the stability and strength prediction of CFS beam-columns were assessed under the actual stress distribution generated by combined actions of compression and bending moment. Li et al. [14] investigated the behaviour of beam-columns under eccentric compressive loads through experimental and numerical investigations and similar conclusions were drawn on the efficiency of the simplified linear interaction formulas. Hasanali et al. [15] conducted an evaluation of both Direct Strength Method (DSM) and existing design proposals in the literature to determine their reliability in estimating the load-carrying capacity of CFS warping-restrained beam-columns. The study findings revealed that the DSM yielded significant conservative predictions for beam-column members, with a deviation of up to 55%. This deviation was attributed to various factors, including the influence of warping-restrained boundary conditions, the accuracy of buckling load calculations, and the effectiveness of the code-prescribed linear interaction formula.

The accuracy of the current design standards, including Australian/New Zealand Standard (AS/NZS 4600) [16], American Iron and Steel Institute (AISI S100) [17], and European design guidelines (EC3) [18-20], in the strength predictions of CFS beam-columns was first evaluated in this study. An empirical nonlinear interaction equation was then proposed to provide more reliable design solutions for the design of CFS beam-column elements with single channel sections. To this end, detailed nonlinear FE models of CFS beam-column members under various load combinations were developed by taking into account material nonlinearity and geometric imperfections and then validated against the results of experimental tests. The validated models were then utilized for a comprehensive parametric study that contains 513 FE models, covering a wide range of key design parameters, such as length, thickness and cross-sectional dimensions under 19 different load eccentricities. Finally, the results were employed to develop a more accurate interaction equation for design of CFS beam-column members.

2 CURRENT DESIGN METHODS FOR CFS BEAM-COLUMNS

Current design guidelines such as AS/NZS 4600 [16] and AISI S100 [17] incorporate the DSM to predict the load-carrying capacity of CFS members, as an alternative to the traditional Effective Width Method (EWM) prescribed by the European design guidelines [18-20].

2.1 Resistance of beam-column elements by interaction expressions

A simplified linear combination of compressive and flexural elastic buckling resistances is employed by AS/NZS 4600 [16] and AISI S100 [17] (Eq. (1) and (Eq. (2)) to design CFS members under the combined effects of the axial compressive loads and bending moments:

$$\frac{N^*}{N_c} + \frac{M_x^*}{M_{bx}} + \frac{M_y^*}{M_{by}} \leq 1.0 \quad (1)$$

$$\frac{P}{P_n} + \frac{M_x}{M_{nx}} + \frac{M_y}{M_{ny}} \leq 1.0 \quad (2)$$

To determine the capacity of the CFS elements under any combination of P, M_x and M_y, interaction equations utilise the anchor points of interaction curves, which are the capacities under pure compression (P_n) and pure bending moments (M_{nx} and M_{ny}). Nominal pure strength (P_n, M_{nx} and M_{ny}) is typically determined by the DSM equations. However, in this study, to assess the efficiency of the interaction equation (Eq. (2)), the inaccuracy of the DSM equations in estimating the pure nominal strength values is excluded from this equation [15]. To this end, the axial compressive strength (P_n) and flexural capacities (M_{nx} and M_{ny}) of the sections, here called nominal pure capacities, are determined using experimentally validated FE models of the CFS elements with warping-restrained boundary conditions (see Section 3).

2.2 European design standard

According to EC3 [18-20], the strength of CFS beam-columns is taken as the minimum of the following two resistances: (i) cross-sectional resistance and (ii) member buckling resistance. As outlined in Clause 8.1.8 of EC3 Part 1-3 [18], the cross-section of a CFS beam-column subjected to the combined action of axial compression (N_{Ed}) and bending moments ($M_{y,Ed}$ and $M_{z,Ed}$) should satisfy the following criteria:

$$\frac{N_{Ed}}{N_{c,Rd}} + \frac{M_{x,Ed} + \Delta M_{x,Ed}}{M_{cx,Rd,com}} + \frac{M_{y,Ed} + \Delta M_{y,Ed}}{M_{cy,Rd,com}} \leq 1.0 \quad (3)$$

The factors $\Delta M_{x,Ed}$ and $\Delta M_{y,Ed}$ are defined as the additional bending moments generated by the shift of the centroidal axes of the effective cross-section relative to those of the gross cross-section, which are estimated by:

$$\Delta M_{x,Ed} = N_{Ed} e_{Ny} \quad (4)$$

$$\Delta M_{y,Ed} = N_{Ed} e_{Nx} \quad (5)$$

With respect to the member resistance, the following interaction equations are recommended by Clause 8.2.5 of EC3 Part 1-3 [18] for two different buckling axes:

(i) Major principal axis buckling:

$$\left(\omega_{z,x} \frac{N_{Ed}}{\chi_x N_{c,Rd}}\right)^{\alpha_x} + \left(\omega_{z,LT} \frac{M_{x,Ed} + \Delta M_{x,Ed}}{\chi_{LT} M_{cx,Rd}}\right)^{\beta_x} + \left(\frac{M_{y,Ed} + \Delta M_{y,Ed}}{M_{cy,Rd}}\right)^{\delta_x} \leq 1.0 \quad (6)$$

(ii) Minor principal axis buckling:

$$\left(\omega_{z,y} \frac{N_{Ed}}{\chi_y N_{c,Rd}}\right)^{\alpha_y} + \left(\omega_{z,LT} \frac{M_{x,Ed} + \Delta M_{x,Ed}}{\chi_{LT} M_{cx,Rd}}\right)^{\beta_y} + \left(\frac{M_{y,Ed} + \Delta M_{y,Ed}}{M_{cy,Rd}}\right)^{\delta_y} \leq 1.0 \quad (7)$$

exponents of Eqs. (6) and (7) (α_x, α_y, β_x, β_y, δ_x and δ_y) are defined according to the following formulas:

$$\alpha_x,\ \beta_x, \delta_x = \chi_x/\omega_{z,x} \geq 0.85$$
$$\alpha_y,\ \beta_y, \delta_y = \chi_y/\omega_{z,y} \geq 0.85 \quad (8)$$

3 FINITE ELEMENT MODEL AND VALIDATION

In this study, to validate detailed nonlinear FE models, the results of an experimental programme conducted by Torabian et al. [21] at Johns Hopkins University on CFS elements under combined axial compression and bending moments were utilized. The main features of the models are briefly summarized as follows.

The boundary conditions of the experimental test set-up were replicated in the FE models, as demonstrated in Fig. 1. Two reference points were placed at the end sections of the lipped channel elements to simulate the support and applied eccentric compression. The nodal degrees of freedoms at each end of the element were then coupled to their respective reference point which was pinned about the minor- and major-axes.

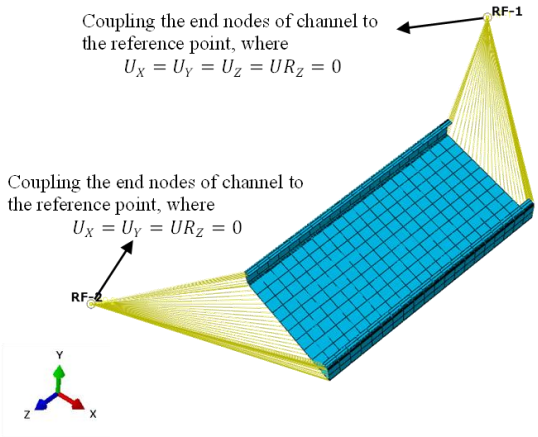

Fig. 1 CFS element boundary conditions under eccentric compressive load

In the present study, a nine-node ABAQUS [23] shell element with reduced integration and using quadratic shape functions, $S9R5$, was used to simulate the behaviour of the CFS beam-column elements. Following a mesh sensitivity analysis, the element size of 10×10 mm^2 was adopted for the flat regions of the CFS beam-columns, whereas four elements were used in the radial direction of their corners.

The engineering stress-strain curves obtained from coupon tests [21] were converted to true stress and true strain data. The engineering and true stress-strain curves of the tested beam-column elements are shown in Fig. 2. The measured Poisson ratio, Young's modulus of elasticity, the yield stress, and the ultimate stress of the CFS material are equal to $\upsilon = 0.3$, E =203.4 GPa, $F_y = 365\ MPa$, and $F_u = 560\ MPa$, respectively.

An elastic eigen buckling analysis was used to generate the initial imperfections. For the CFS element with a thickness (t) smaller than 3 mm, the magnitude of the buckled shape was scaled to 0.34t and 0.94t for local and distortional buckling, respectively, according to Schafer and Peköz [24]. For the specimens with a thickness (t) exceeding 3 mm, the imperfection magnitude was determined using the equation proposed by Walker [25].

Table 1 lists the cross-sectional dimensions and lengths of the beam-column specimens subjected to eccentric compressive loads with nine different eccentricity values on the major- (x) and minor- (y) axes, as well as their strengths obtained from the FE simulations and the tests [21]. In general, a good agreement can be seen between the predicted strength by FE

models (P_{DFE}) and those extracted from tests (P_{Test}) with a maximum estimation error of 4% and a standard deviation of 0.02 (see Table 1).

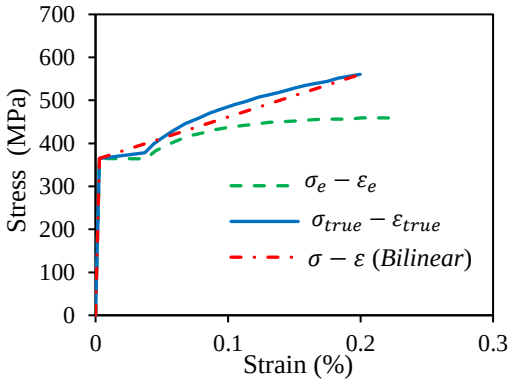

Fig. 2 Material stress-strain relationship used in FE models

Table 1 Comparison between CFS beam-column strength under various eccentric compressive loads obtained from reference experimental tests (P_{Test}) and FE models (P_{FE})

Specimen label	Length	Cross-sectional geometry dimensions	Eccentricities		Capacities		$\frac{P_{Test}}{P_{FE}}$
	$L\ (mm)$	(mm)	e_x (mm)	e_y (mm)	P_{Test} (kN)	P_{FE} (kN)	
S600-12-1		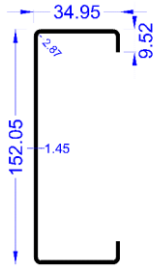	-25.4	0	25.4	25.5	1.00
S600-12-11	305		0	-191	20.6	20.2	1.02
S600-12-15			15.24	-76.2	25.0	26.1	0.96
S600-24-5			15.24	0	25.0	24.6	1.02
S600-24-8	610		0	-76.2	34.8	35.5	0.98
S600-24-15			-14.2	-69.9	25.0	25.4	0.98
S600-48-1			-38.1	0	11.1	11.3	0.98
S600-48-9	1219		0	-140	23.4	23.0	1.02
S600-48-15			-13	-63.5	17.6	17.4	1.01
Average					23.1	23.2	1.00
Standard Deviation					6.46	6.67	0.02

* Negative eccentricity in the x direction shows that the web of the specimens is in compression.

4 PARAMETRIC STUDY

A comprehensive parametric study was conducted, using the experimentally validated FE models described in the previous section, to investigate the efficiency of the code-prescribed compressive load-bending moment interaction equations and develop a more accurate interaction formulation for the CFS beam-columns. The compiled dataset consisted of a range of key design variables, including three sets of cross-sectional dimensions ($Ch.1$, $Ch.2$ and $Ch.3$), thicknesses (1 mm, 2 mm and 4 mm) and lengths (500 mm (short), 1500 mm (medium) and 3000 mm (long)), as shown in Table 4. In addition, the effects of all possible combinations of axial compressive load and bending moments were evaluated by selecting 19 different combinations of loading conditions, as shown in Table 3. The mechanical properties of the CFS material were taken as $F_y = 440\ MPa$, $F_u = 600\ MPa$, $E = 207\ GPa$ and $\vartheta = 0.3$.

Table 2 Parametric study variables

Section geometry	Section name		
	$Ch.1$	$Ch.2$	$Ch.3$
Web height (h (mm))	300	250	200
Flange (b_f (mm))	50	75	100
Lip (d_1 (mm))	25		
Thickness (t (mm))	1, 2 and 4		
Length (L (mm))	500, 1500 and 3000		

Table 3 Magnitude of the eccentricities

Eccentricities	Loading condition																		
	Pure actions				Combined actions														
	P	M_x	M_y	M_y	$P+M_y$						$P+M_x$			$P+M_x+M_y$					
e_x (mm)	0	0	-∞	∞	10	-10	25	-25	50	-50	0	0	0	10	-10	25	-25	50	-50
e_y (mm)	0	∞	0	0	0	0	0	0	0	0	10	100	200	10	10	100	100	200	200

5 RESULTS AND DISCUSSIONS

The behaviour of the CFS elements was first assessed by using normalised two-dimensional (2D) strength interaction surfaces ($P-M$) under combinations of compression load and bending moments about either a major- or minor-axis. The capacities of the beam-columns were then examined to determine the accuracy of the interaction equation (Eq. (2)) prescribed in AS/NZS 4600 [16] and AISI S100 [17] as well as EC3 guidelines [18] under all selected eccentricities. Following that, by using an optimisation process, the errors between the results of the detailed FE models and the strength values estimated from the proposed equation (P_{Prop}) were minimised to develop a more accurate interaction equation for the design of CFS beam-columns.

5.1 Assessment of beam-columns under major-axis bending

Fig. 3 illustrates the normalised peak compressive loads (P/P_n) and major-axis bending moments (M_x/M_{nx}) obtained from the validated FE models in the 2D interaction space. Based on the element slenderness ratios about the minor-axis (λ_y), the data points were divided into three categories: (i) low $\lambda_y \leq 50$ (see Fig. 3(a)), (ii) medium $50 < \lambda_y \leq 100$ (see Fig. 3(b)) and (iii) high $\lambda_y > 100$ (see Fig. 3(c)). It should be noted that $\lambda_y = KL/r_y$, where r_y, L and K are defined as the radius of gyration about the minor-axis, unbraced length of the member and effective length factor, respectively.

It can be seen from Fig. 3(a) that the code-prescribed interaction curve (Eq. (2)) may lead to either underestimated or overestimated strength predictions for the CFS elements with low slenderness ratios (i.e., $\lambda_y \leq 50$), while on average provides reasonable predictions. In general, it is evident that the interaction equation could predict the strength of the beam-columns under low eccentricities with a higher level of accuracy compared to those under larger eccentricities. Fig. 3(b) indicates that the interaction equation (Eq. (2)) provided conservative estimations of the strength of CFS beam-columns with medium slenderness ratios (i.e., $50 < \lambda_y \leq 100$) as the data points generally fell above the Eq. (2). In contrast, it can be seen from Fig. 3(c) that the strength of CFS beam-columns with high slenderness ratios (i.e., $\lambda_y > 100$) was always underestimated by using the code-prescribed interaction equation.

5.2 Beam-columns in a $P-M_y$ space

The behaviour of the CFS beam-columns subjected to the combined compressive load and minor-axis bending moment is investigated in this section. In this case, it was found that categorizing the data points based on the cross-sectional web slenderness ratio (h/t) helps in a better understanding of the beam-column behaviour. Thereby, the specimens were divided into three categories: (i) low web slenderness ratio h/t <100 (see Fig. 4(a)), (ii) medium web slenderness ratio 100≤ h/t <200 (see Fig. 4(b)) and (iii) high web slenderness ratio h/t ≥200 (see Fig. 4(c)).

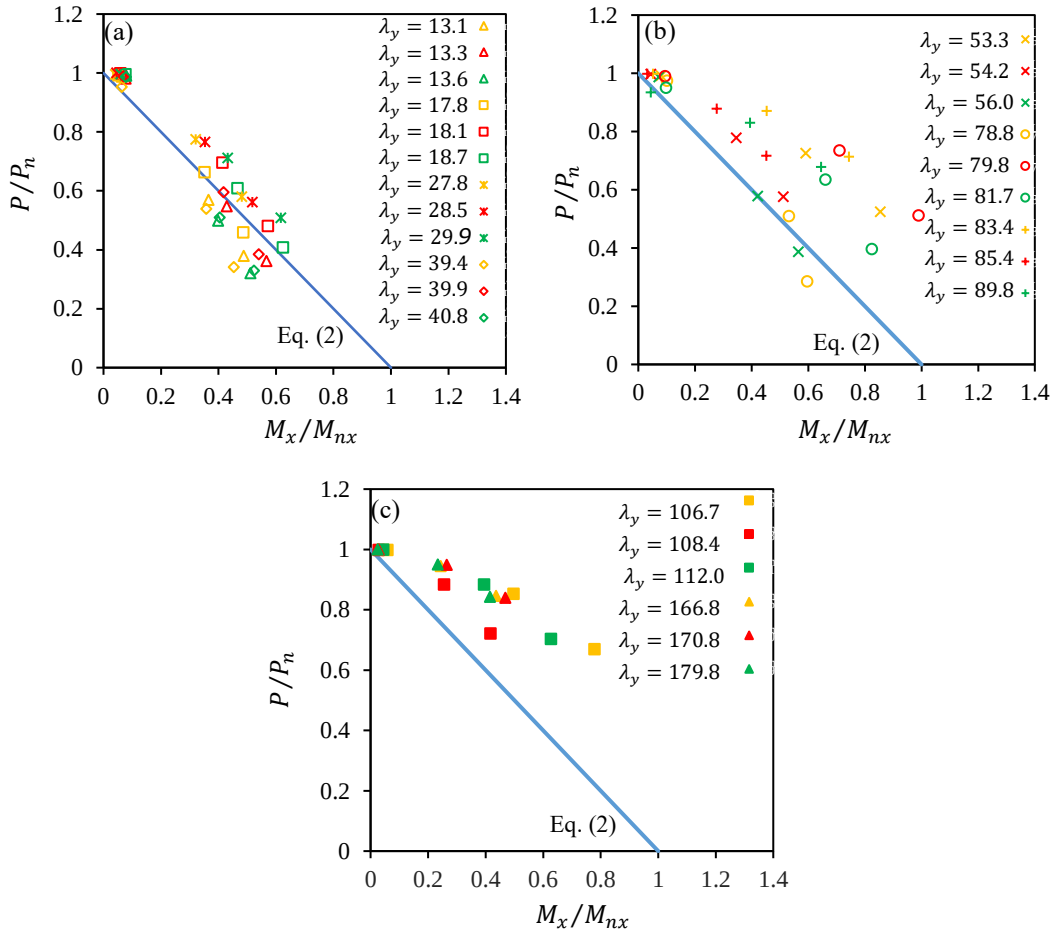

Fig. 3 Interaction of P/P_n and M_x/M_{nx} for CFS beam-columns with (a) low slenderness ($\lambda_y \leq 50$), (b) medium slenderness ($50 < \lambda_y \leq 100$), and (c) high slenderness ($\lambda_y > 100$).

It can be seen from Fig. 4(a) that almost all data points belonging to the elements with the low web slenderness (i.e., h/t <100) were positioned below the interaction curve (Eq. (2)). This implies that using the proposed interaction equation in AISI S100 [17] leads to unsafe strength predictions of the low web slenderness elements subjected to compression and minor-axis bending. On the other hand, for the specimens with the medium (Fig. 4(b)) and high (Fig. 4(c)) web slenderness, Eq. (2) led to either underestimated or overestimated results, mainly when combined compression and positive minor-axis bending or combined compression and negative minor-axis bending was imposed, respectively.

5.3 Evaluation of the code-prescribed interaction expressions

As outlined in Section 2.1, the axial compressive strength (P_n) and flexural capacities (M_{nx} and M_{ny}) of the sections, here called nominal pure capacities, were determined using

experimentally validated FE models of the CFS elements with warping-restrained boundary conditions. The predicted P_n, M_{nx} and M_{ny} obtained from FE analyses are listed in Table 4.

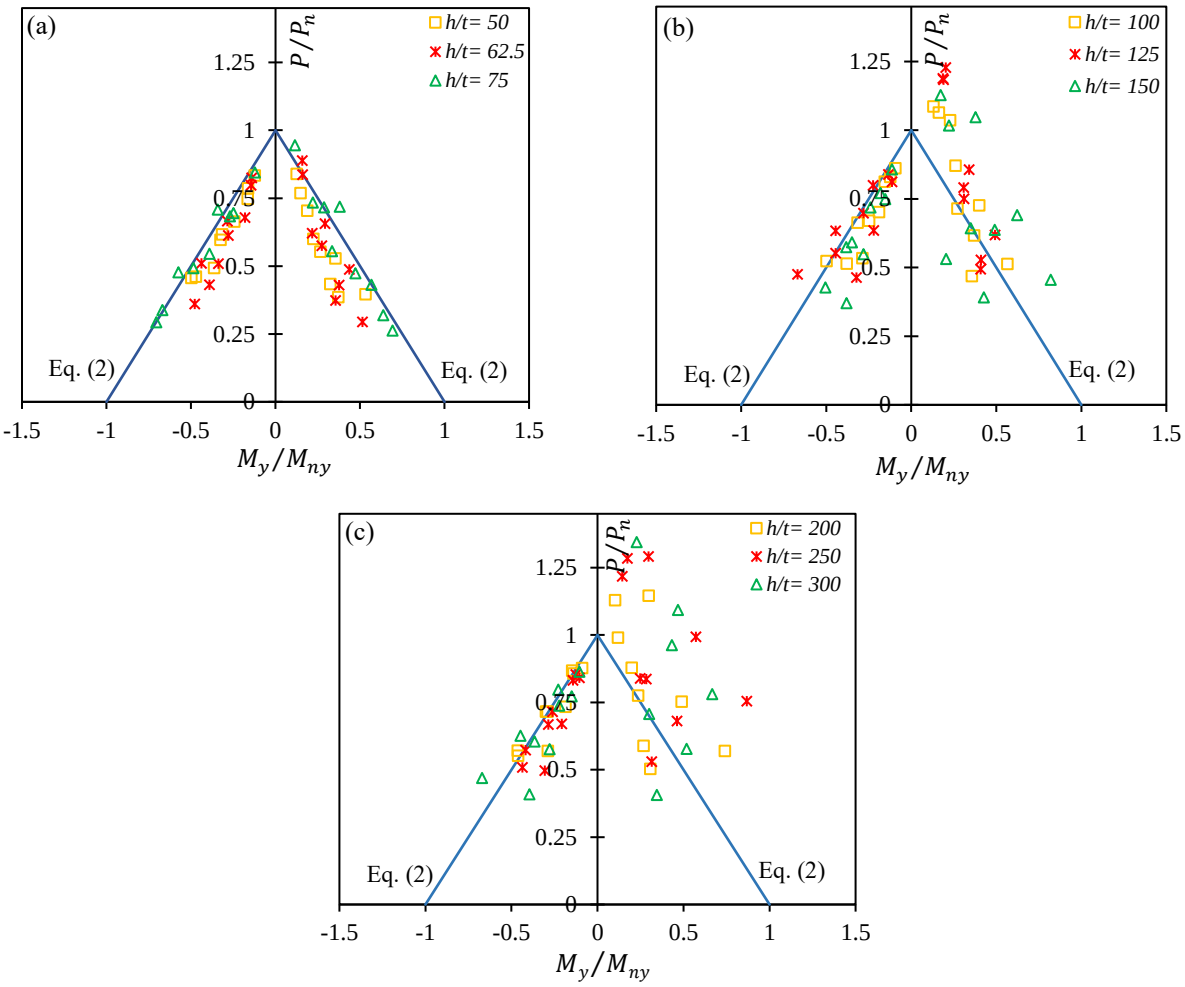

Fig. 4 Interaction of P/P_n and M_y/M_{ny} for CFS beam-columns with (a) low web slenderness ($h/t < 100$), (b) medium web slenderness ($100 \leq h/t < 200$), and (c) high web slenderness ($h/t \geq 200$).

Table 4 Nominal pure strengths of the CFS elements

Section name	Length	Thickness	Compression	Major-axis bending	Minor-axis bending (Web in compression)	Minor-axis bending (Web in tension)
	$L\ (mm)$	$t\ (mm)$	$P_n\ (kN)$	$M_{nx}\ (kN.m)$	$M_{ny}\ (kN.m)$	$M_{ny}\ (kN.m)$
$Ch.1$	500	1	43.3	10.4	2.2	2.5
		2	139.1	30.2	6.8	6.4
		4	393.6	64.8	8.2	7.5
	1500	1	28.6	5.5	1.0	1.6
		2	83.0	26.3	3.5	2.3
		4	224.4	47.2	5.7	5.6
	3000	1	13.9	5.4	1.2	0.8
		2	35.8	12.9	2.7	2.3
		4	77.0	31.3	5.4	6.4
$Ch.2$	500	1	49.9	9.4	4.1	4.2
		2	172.8	29.0	12.4	11.1
		4	487.8	63.6	26.9	25.6
	1500	1	42.1	5.2	2.5	3.1
		2	132.7	29.9	4.7	8.0
		4	477.3	65.4	18.0	13.7
	3000	1	27.4	4.7	1.9	1.2
		2	76.1	26.3	4.7	4.8
		4	189.5	42.4	11.1	10.6
$Ch.3$	500	1	53.5	8.3	5.3	5.8
		2	195.5	25.0	18.2	16.2
		4	574.5	71.9	39.1	38.4
	1500	1	50.0	7.5	3.0	4.1
		2	174.8	24.9	11.8	11.4
		4	520.2	65.5	25.5	26.9
	3000	1	39.9	3.8	2.5	1.5
		2	128.2	13.2	6.7	5.8
		4	374.4	35.9	17.2	13.9

In comparison to the strength predictions of the detailed FE models (P_{FE}) and the interaction equation prescribed in AISI (P_{Code}), it was concluded that regardless of the imposed bending moment direction, the interaction equation may provide unsafe strength predictions for the elements with low slenderness ratios ($\lambda_y \leq 50$) by up to 37.2%. On the contrary, the capacities of the beam-columns with medium and high slenderness ratios ($\lambda_y > 50$) were generally underestimated (up to 41.1%) by the code proposed interaction equation in AS/NZS 4600 [16] and AISI S100 [17] (more comprehensive details can be found in [22]).

With respect to the accuracy of the EC3 [18] design guidelines in predicting the strength of CFS beam-column elements (P_{EC3}), it was revealed that there is a good agreement between the strength of CFS beam-columns with low slenderness ($\lambda_y \leq 50$) and those obtained from the validated FE models (P_{FE}) with an average error of 9.2%. On the other hand, EC3 [17] strength predictions for medium to high slenderness elements ($\lambda_y > 50$) resulted in an average error of 15.6% compared to the FE results.

6 DEVELOPMENT OF DESIGN EQUATIONS

To improve the strength predictions of the CFS beam-columns, a general trinomial expansion was proposed for the interaction equation by taking into account the effects of the element slenderness ratio (λ_y) and web slenderness ratio (h/t) as the key parameters identified in the previous sections. It is worth noting that the effects of these parameters on the behaviour of the beam-columns have not been considered in the code-proposed equations as well as in the literature.

$$(\frac{P}{P_n})^{\alpha} + (\frac{M_x}{M_{nx}})^{\alpha} + (\frac{M_y}{M_{ny}})^{\alpha} \leq 1.0 \tag{9}$$

where

$$\begin{cases} \alpha = 0.95 & For\ \lambda_y \leq\ 50\ (low\ slenderness) \\ \alpha = 1 + \dfrac{h/t}{1000} & For\ \lambda_y > 50\ (medium/high\ slenderness) \end{cases} \tag{13}$$

Using an iterative optimisation process, the factor α was obtained for low, medium, and high slenderness elements by minimising the errors between the strength results obtained from the proposed equation (P_{Prop}) and the detailed FE models (P_{FE}) calculated by the following equation:

$$Error = \Sigma \left(1 - \frac{P_{prop}}{P_{FE}}\right)^2 \tag{14}$$

The data points were divided into various categories in terms of element slenderness ratio about the minor-axis ($\lambda_y = KL/r_y$) and cross-sectional web slenderness ratio (h/t) to find the best correlation between the actual and the predicted values. The optimum results of the different categories led to the most efficient α variable for Eq. (12) as illustrated in Fig. 5. The presented results are the average α values for each category of the λ_y comprising various h/t ratios. The factor α was kept constant for the elements with low slenderness ratios ($\lambda_y \leq 50$) as h/t exhibited a negligible contribution to the α values (see Fig. 5(a)). However, for the other elements with medium and high slenderness ratios ($\lambda_y >50$), a linear correlation was observed between the calculated α and h/t of the section (see Fig. 5(b)).

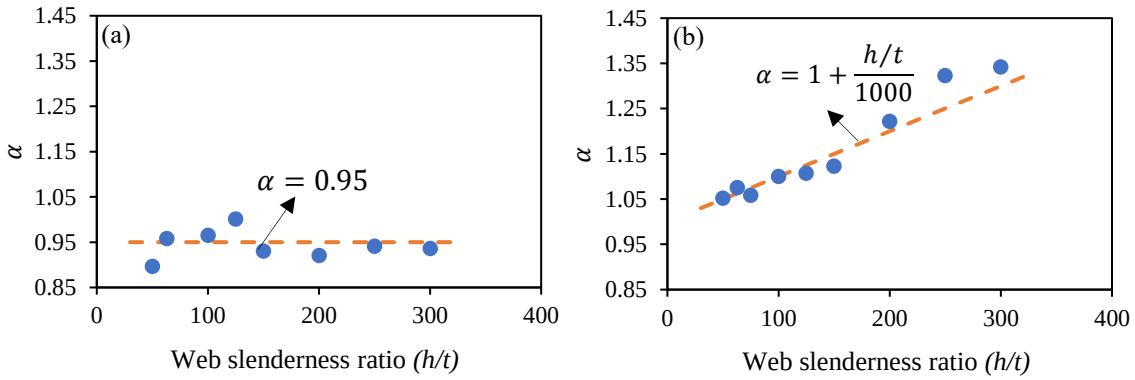

Fig. 5 α factor versus web slenderness ratios for the CFS elements with (a) $\lambda_y \leq 50$ and (b) $\lambda_y > 50$

Table 5 lists the average errors associated with the strength predictions obtained using the design guidelines outlined in AS/NZS 4600 [16] and AISI S100 [17] and (P_{code}) and EC3 [18] (P_{EC3}), as well as the interaction equation proposed in this study (P_{Prop}). The results indicate that the proposed interaction equation, on average, could improve the accuracy of the code strength predictions, especially in the case of medium to high slenderness elements.

For the low-slenderness CFS beam-columns, all design regulations resulted in an almost similar average error of around 9%. The interaction equations prescribed in EC3 [17] (Eqs. (6) and (7)), however, led to more conservative strength values for CFS elements with medium and

high slenderness compared to the other methods. In the case of medium to high slenderness beam-columns, the average errors of the interaction equations prescribed by AS/NZS 4600 [16] and AISI S100 [17] (Eq. (2)) as well as EC3 Part 1-3 [18] (Eqs. (6) and (7)) were reduced from 12.4% and 15.6%, respectively, to less than 10% by using the proposed equation. The results also indicate that the improvement in the accuracy is more evident in the case of CFS elements with medium and high slenderness ratios.

Table 5 Average error (%) associated with strength predictions of each method compared to the FE results

Member slenderness ratio	P_{code} *vs* P_{FE}	P_{EC3} *vs* P_{FE}	P_{Prop} *vs* P_{FE}
$\lambda_y \leq 50$	9.4	9.2	9.0
$\lambda_y > 50$	12.4	15.6	9.8

7 SUMMARY AND CONCLUSION

The main objective of this paper was to develop the accuracy of the linear interaction equations prescribed by AS/NZS 4600 [16] and AISI S100 [17] for design of CFS single section beam-column elements. For this purpose, experimentally validated FE models of CFS beam-columns taking into account the geometric imperfections and the material non-linearity were employed to conduct a comprehensive parametric study. The prepared dataset covered an extensive range of key design, including different cross-sectional geometries, lengths as well as directions and values of load eccentricity levels. The results were then used to assess the accuracy of the current design specifications, including AS/NZS 4600 [16], AISI S100 [17], and EC3 [18] in predicting the compressive capacity of the CFS beam-columns. Subsequently, by minimizing the errors between the strength results obtained from the validated FE models and the predicted values using an iterative optimisation method, a general trinomial expansion was proposed for the interaction equation, as a function of element and web slenderness ratios. Based on the presented results, the following conclusions were drawn:

- The accuracy of the interaction equations specified in the design codes is influenced by the following three main factors: (i) element slenderness ratio (λ_y), (ii) web slenderness ratio (h/t) and (iii) the value and direction of the eccentricities (e_y and e_x).
- The current design regulations resulted in an almost similar average error of around 9% for low-slenderness CFS beam-column elements ($\lambda_y \leq 50$). In the case of medium to high slenderness elements ($\lambda_y > 50$), however, the EC3 interaction equations [17] provided the most conservative predictions with the average error of 15.6%.
- For CFS beam-column elements characterised by low slenderness ratios ($\lambda_y \leq 50$), the α factor for the proposed interaction equation closely resembles the prescribed interaction equations outlined in AS/NZS 4600 [16] and AISI S100 [17]. However, in the case of medium to high slenderness ($\lambda_y > 50$) elements, the average errors of AS/NZS 4600 [16] and AISI S100 [17] (Eq. (2)) and EC3 Part 1-3 [18] (Eqs. (6) and (7)) predictions were reduced from 12.4% and 15.6%, respectively, to 9.8% through the utilisation of the proposed equation.

REFERENCES

[1] Hasanali, Maryam, Krishanu Roy, Seyed Mohammad Mojtabaei, Iman Hajirasouliha, G. Charles Clifton, and James BP Lim. "A critical review of cold-formed steel seismic resistant systems: Recent developments, challenges and future directions." *Thin-Walled Structures* 180 (2022): 109953.

[2] Mojtabaei, Seyed Mohammad, Jurgen Becque, and Iman Hajirasouliha. "Structural Size Optimization of Single and Built-Up Cold-Formed Steel Beam-Column Members." *Journal of Structural Engineering* 147, no. 4 (2021): 04021030.

[3] Torabian, Shahabeddin, and Benjamin W. Schafer. "Development and experimental validation of the Direct Strength Method for cold-formed steel beam-columns." *Journal of Structural Engineering* 144, no. 10 (2018): 04018175.

[4] Torabian, Shahabeddin, Baofeng Zheng, and Benjamin W. Schafer. "Experimental response of cold-formed steel lipped channel beam-columns." *Thin-walled structures* 89 (2015): 152-168.

[5] Torabian, Shahabeddin, David C. Fratamico, and Benjamin W. Schafer. "Experimental response of cold-formed steel Zee-section beam-columns." *Thin-walled structures* 98 (2016): 496-517.

[6] Papargyriou, Ioannis, and Iman Hajirasouliha. "More efficient design of CFS strap-braced frames under vertical and seismic loading." *Journal of Constructional Steel Research* 185 (2021): 106886.

[7] Papargyriou, Ioannis, Iman Hajirasouliha, Jurgen Becque, and Kypros Pilakoutas. "Performance-based assessment of CFS strap-braced stud walls under seismic loading." *Journal of Constructional Steel Research* 183 (2021): 106731.

[8] Mojtabaei, Seyed Mohammad, Jurgen Becque, and Iman Hajirasouliha. "Local buckling in cold-formed steel moment-resisting bolted connections: behavior, capacity, and design." *Journal of Structural Engineering* 146, no. 9 (2020): 04020167.

[9] Mojtabaei, Seyed Mohammad, Jurgen Becque, and Iman Hajirasouliha. "Behavior and Design of Cold-Formed Steel Bolted Connections Subjected to Combined Actions." *Journal of Structural Engineering* 147, no. 4 (2021): 04021013.

[10] CEN (European Committee for Standardization). *Eurocode 3: Design of steel structures—Part 1–1: General rules and rules for buildings*. Brussels, Belgium: CEN, 2005.

[11] CEN (European Committee for Standardization). *Eurocode 3: Design of steel structures—Part 1–3: General rules- Supplementary rules for cold formed members and sheeting*. Brussels, Belgium: CEN, 2005.

[12] Hancock, G. J., and K. J. R. Rasmussen. "Recent research on thin-walled beam-columns." *Thin-Walled Structures* 32, no. 1-3 (1998): 3-18.

[13] Cheng, Shan-shan, Boksun Kim, and Long-yuan Li. "Lateral–torsional buckling of cold-formed channel sections subject to combined compression and bending." *Journal of Constructional Steel Research* 80 (2013): 174-180.

[14] Li, Yuanqi, Yinglei Li, and Yanyong Song. "Experimental investigation on ultimate capacity of eccentrically-compressed cold-formed beam-columns with lipped channel sections." Paper presented at 22nd International Specialty Conference on Cold-Formed Steel Structures, St. Loius, 2014.

[15] Hasanali, Maryam, Seyed Mohammad Mojtabaei, G.Charles Clifton, Iman Hajirasouliha, Shahabbeddin Torabian and James B.P.Lim. "Capacity and design of cold-formed steel warping-restrained beam-columns." *Journal of Constructional Steel Research* 190 (2022): 107139.

[16] AS/NZS 4600 (Australian Standard/New Zealand Standard). *Cold-formed steel structures*. Sydney/Wellington, 2018.

[17] AISI (American Iron and Steel Institute). *North American specification for the design of cold-formed steel structural members* (AISI S100-16). Washington, DC: AISI, 2016.

[18] CEN (European Committee for Standardization). *Eurocode 3: Design of steel structures-Part 1-3: General rules: Supplementary rules for cold-formed members and sheeting*. Brussels, 2022.

[19] CEN (European Committee for Standardization). *Eurocode 3: Design of steel structures-Part 1-1: General rules and rules for buildings*. Brussels, 2020.

[20] CEN (European Committee for Standardization). *Eurocode 3: Design of steel structures-Part 1-5: Plated structural elements*. Brussels, 2020.

[21] Torabian, Shahabeddin, Baofeng Zheng, and B. W. Schafer. "Direct strength prediction of cold-formed steel beam-columns." *Research Rep. RP16-3. Ithaca, NY: American Iron and Steel Institute* (2016).

[22] Hasanali, Maryam, Seyed Mohammad Mojtabaei, Iman Hajirasouliha, G. Charles Clifton, and James BP Lim. "More accurate design equations for cold-formed steel members subjected to combined axial compressive load and bending." *Thin-Walled Structures* 185 (2023): 110588. https://doi.org/10.1016/j.tws.2023.110588

[23] Abaqus/CAE User's Manual, version 6.23, USA, (2021).

[24] Schafer, Benjamin W., and Teoman Peköz. "Computational modeling of cold-formed steel: characterizing geometric imperfections and residual stresses." *Journal of* constructional *steel research* 47, no. 3 (1998b): 193-210. https://doi.org/10.1016/S0143-974X(98)00007-8

[25] Walker, A. C. (Ed.). (1975). *Design and analysis of cold-formed sections*. John Wiley & Sons.